09

Electron-nuclear interaction of boron vacancies in hexagonal boron nitride

© E.V. Dmitrieva[1], G.V. Mamin[1], F.F. Murzakhanov[1], I.N. Gracheva[1], M.R. Gafurov[1], V.A. Soltamov[2]

[1] Kazan Federal University,
Kazan, Tatarstan, Russia
[2] Ioffe Institute,
St. Petersburg, Russia
E-mail: ev600@mail.ru

Received April 30, 2025
Revised September 8, 2025
Accepted November 11, 2025

The interactions of a spin defect and nearby nitrogen nuclei in hexagonal boron nitride have been studied by electron paramagnetic resonance and double electron-nuclear resonance. The constants of the hyperfine ($A_{iso} = 59.5$ MHz, $A_{dd} = 13.8$ MHz) and quadrupole ($C_q = 1.96$ MHz) interactions for nitrogen nuclei ^{14}N of the first coordination sphere are determined. The results obtained are important for understanding the mechanisms of electron-nuclear interactions in hBN and for developing quantum devices based on spin defects in two-dimensional materials.

Keywords: electron paramagnetic resonance, ENDOR spectroscopy, boron vacancy, hBN, spin defect.

DOI: 10.61011/PSS.2025.12.63113.8056k-25

1. Introduction

A feature of the studied spin defects for quantum applications is their ability to maintain quantum coherence at room temperature ($T = 297$ K), which has been experimentally confirmed by optically detectable magnetic resonance methods. The above-mentioned advantage radically distinguishes the system under study from traditional superconducting qubits requiring low temperatures (~ 10 mK), which presents additional difficulties in scaling and implementing quantum algorithms. The electron spin-spin relaxation time T_2 of the boron vacancy is estimated to be on the order of several microseconds [1–4].

A negatively charged boron vacancy V_B^- in a hexagonal boron nitride (hBN) crystal is a Frenkel point defect with local symmetry D_{6h} surrounded by three equivalent nitrogen atoms in the plane of the BN layer, which occurs when a boron atom is removed during irradiation with high-energy particles followed by electron capture from the crystal lattice [5]. The spin defect V_B^- is of particular value for quantum computing due to its unique spin and optical properties. An important condition for the applicability of the qubit is the possibility of initializing, reading, and manipulating spin states. These operations can be implemented by combined optical, microwave, and radio frequency effects for boron vacancy states in hBN [6–8].

However, there are stricter requirements for coherence times, since this parameter defines the time interval for performing quantum operations and storing quantum information [9]. A long coherence time of nuclear spins on the order of milliseconds [10] is critically important for the implementation of quantum memory and electronic nuclear registers [11,12], where nuclear spins act as long-lived memory elements, and electronic spins provide a control channel. Thus, it becomes necessary to obtain quantities characterizing the nuclei and their interactions with the boron vacancy.

2. Details of the experiment

In this work, we studied a single crystal of hexagonal boron nitride with a size of $0.90 \times 0.54 \times 0.05$ mm, exposed to an electron beam with an energy of 2 MeV. Electron paramagnetic resonance (EPR) experiments were performed on a Bruker Elexsys E680 spectrometer in the W-band (94 GHz) with optical excitation using a diode laser ($\lambda 532$ nm, $P = 100$ mW). In order to obtain the constants of the hyperfine and quadrupole interactions between the spin defect and nitrogen nuclei of the first coordination sphere (Figure 1, *a*), electron nuclear double resonance (ENDOR) spectroscopy was used.

3. Results and their discussion

Two transitions are observed in the spectrum of electron paramagnetic resonance (Figure 1, *b*) corresponding to the fine structure of the boron vacancy with spin $S = 1$. The simulation of the angular dependence of the spectra made it possible to determine the parameters of the spin Hamiltonian. The value of the g-factor was 2.004. Splitting in a zero magnetic field is described by the expression $2D/g\mu_B$ with the value $D = 3.55$ GHz [6].

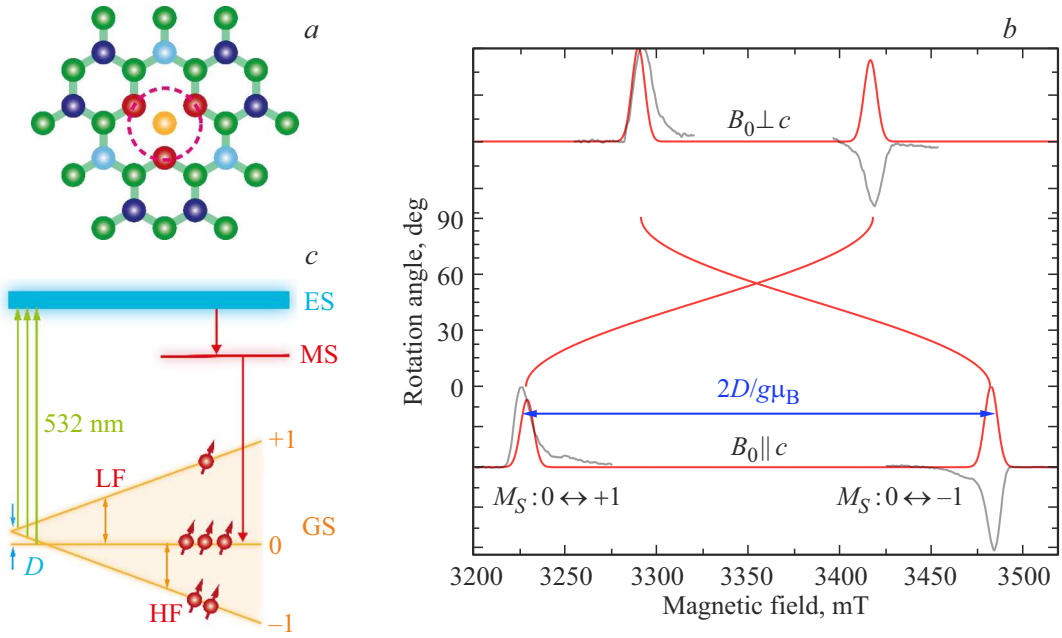

Figure 1. *a* — the hBN crystal lattice, the boron vacancy is depicted in the center.The boron atoms are shown in green, and the nitrogen atoms of the first coordination sphere are shown in red; *b* — the EPR spectrum (black line) and modeling (red line) for two orientations: the c axis of the crystal is parallel and perpendicular to the magnetic field vector B_0 (W is the range, $T = 25$ K). The angular dependence is modeled (solid red lines); *c* — simplified diagram of the energy levels of a spin defect during optical pumping at a wavelength of 532 nm. ES — excited state, MS — metastable state, GS — ground state.

The phase change of the high-field transition signal in the EPR spectrum at 180° is of particular interest, which indicates a deviation of the populations of the spin sublevels from the Boltzmann distribution. This effect is caused by laser pumping and can be interpreted within the framework of the given model of energy levels (Figure 1, *c*) and the corresponding optical transitions.

The spectroscopic features of the system under study are due to a combination of five contributions: electron Zeeman, zero magnetic field splitting, nuclear Zeeman, hyperfine, and quadrupole interactions. The spin Hamiltonian in the case of parallel orientation can be written as follows:

$$\hat{H} = g\mu_B B_0 S_z + D\left(S_z^2 - \frac{S(S+1)}{3}\right) - \gamma\hbar B_0 I_z + \sum_{i=1}^{3}\left(A_{xx}S_x I_{x(i)} + A_{yy}S_y I_{y(i)} + A_{zz}S_z I_{z(i)} + \frac{C_q}{4I(2I-1)}\left(3I_{z(i)}^2 - I(I+1) + \eta(I_{x(i)}^2 - I_{y(i)}^2)\right)\right),$$

where the summation is based on nitrogen nuclei.

For transitions $0 \leftrightarrow +1$ and $0 \leftrightarrow -1$, ENDOR spectra were obtained from nuclei ^{14}N ($I = 1$, 99.6 %) of the first coordination sphere (Figure 2). As a result of the simulation, the main values of the hyperfine interaction tensor were established: $A_{xx} = 46.5$ MHz, $A_{yy} = 45.0$ MHz, $A_{zz} = 87.0$ MHz, which corresponds to the isotropic component $A_{iso} = 59.5$ MHz and the anisotropic contribution $A_{dd} = 13.8$ MHz. The quadrupole coupling constant was $C_q = 1.96$ MHz, and the asymmetry parameter was $\eta = -0.07$. The analysis of spectral features required the application of second-order perturbation theory, which made it possible to explain the observed shifts of the ENDOR signals relative to the Larmor nuclear frequency.

Resonant peaks were found in the perpendicular orientation for the low-field transition near the Larmor frequency (Figure 3). The simulation made it possible to identify the origin of the signals corresponding to the transitions associated with the interactions of the nuclei of the first coordination sphere and the boron vacancy.

The analysis of multicomponent ENDOR spectra made it possible to characterize in detail the radio frequency transitions associated with the ^{14}N nuclei in the first coordination sphere of the boron vacancy in hBN. The dependence of the position of the resonance lines on the spatial orientation (θ, φ) between the boron vacancy and the nearest nitrogen nuclei has been established. The use of exciting pulses opens up the possibility of selective spin control for specific nuclei ^{14}N, in particular, suppressing, if necessary, undesirable nuclear interactions in the system through selective saturation of specific junctions [4]. The analysis of the hyperfine interaction constants showed that the isotropic component significantly exceeds the anisotropic contribution, which indicates a high degree of localization of the spin density on nitrogen atoms. Of particular interest is the possibility of creating hybrid quantum systems where the electron spin acts as a control qubit, and the nuclear spins ^{14}N perform

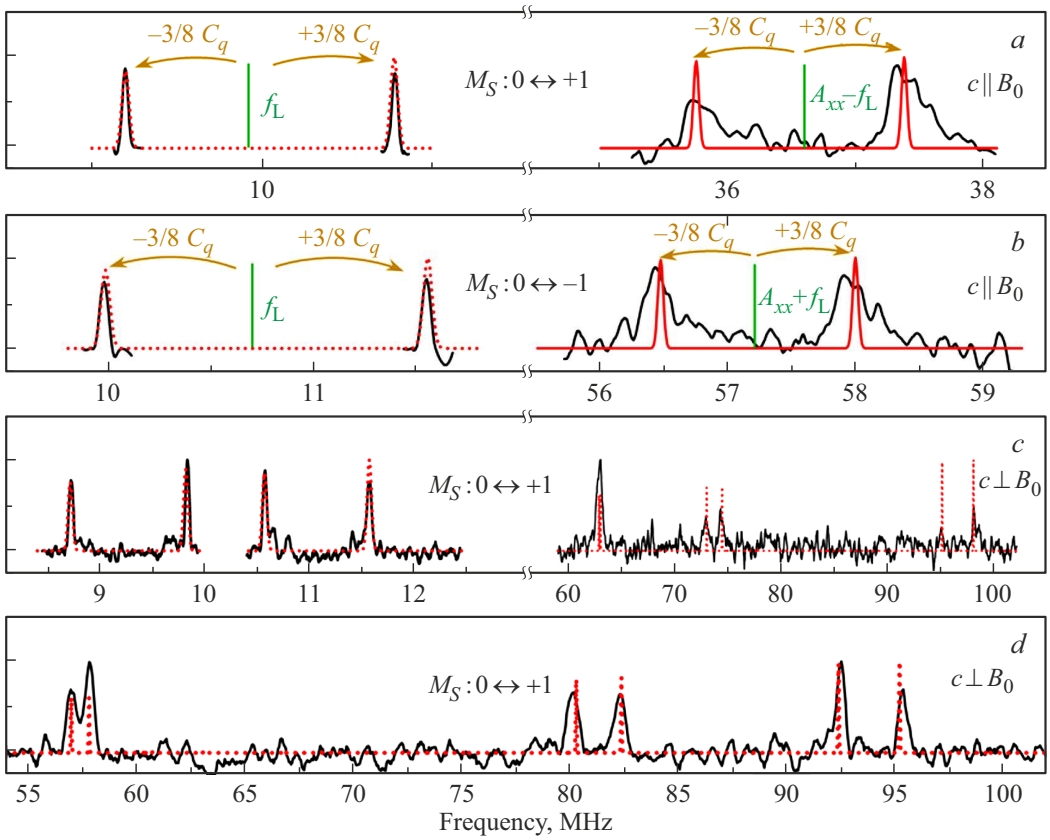

Figure 2. ENDOR spectrum of nitrogen ^{14}N for two electronic transitions: $M_S = 0 \leftrightarrow +1$ in a magnetic field $B_0 = 3223.1$ mT and $M_S = 0 \leftrightarrow -1$ in a magnetic field $B_0 = 3480.5$ mT: *a* — parallel orientation, low-field transition; *b* — parallel orientation, high-field transition; *c* — perpendicular orientation, $\varphi = 7.5°$, $T = 50$ K; *d* —$\varphi = 18°$, $T = 25$ K, where φ is the angle of deflection in the plane of the broken connection. f_L — Larmor frequency of nitrogen ^{14}N, C_q — quadrupole coupling constant.

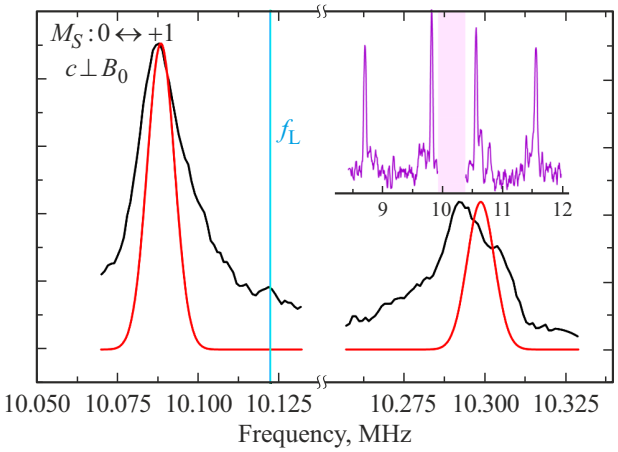

Figure 3. Nitrogen ENDOR spectrum of nitrogen ^{14}N near the Larmor frequency for the transition $M_S = 0 \leftrightarrow +1$ ($\varphi = 7.5°$, $T = 25$ K).

the function of quantum memory. This approach, implemented in a two-dimensional material, opens up new opportunities for the development of scalable quantum devices [13].

4. Conclusion

The conducted studies by the ENDOR spectroscopy method allowed us to study in detail the interaction of the spin defect and the nuclear subsystem. The results obtained open up prospects for the creation of scalable quantum devices based on hybrid electron-nuclear systems, spin defect and cores in hBN can serve as a platform for implementing multi-qubit logical operations and quantum memory with extended coherence time. Further studies may be aimed at optimizing spin state control methods and integrating these systems into practical quantum applications.

Funding

The study was carried out within the framework of the Russian Science Foundation grant No.24-12-00151.

Conflict of interest

The authors declare that there is no conflict of interest.

References

[1] A. Gottscholl, M. Diez, V. Soltamov, C. Kasper, A. Sperlich, M. Kianinia, C. Bradac, I. Aharonovich, V. Dyakonov. Sci. Adv. **7**, *14*, eabf3630 (2021). DOI: 10.1126/sciadv.abf3630

[2] F.F. Murzakhanov, G.V. Mamin, S.B. Orlinskii, U. Gerstmann, W.G. Schmidt, T. Biktagirov, I. Aharonovich, A. Gottscholl, A. Sperlich, V. Dyakonov, V.A. Soltamov. Nano Lett. **22**, *7*, 2718 (2022). DOI: 10.1021/acs.nanolett.1c04610

[3] P. Krantz, M. Kjaergaard, F. Yan, T.P. Orlando, S. Gustavsson, W.D. Oliver. Appl. Phys. Rev. **6**, *2*, 021318 (2019). DOI: 10.1063/1.5089550

[4] J. Lee, H. Park, H. Seo. npj 2D Mater. Appl., **6**, *1*, 60 (2022). DOI: 10.1038/s41699-022-00336-2

[5] G. Barcza, V. Ivády, T. Szilvási, M. Vörös, L. Veis, Á. Gali, Ö. Legeza. J. Chem. Theory Comput. **17**, *2*, 1143 (2021). DOI: 10.1021/acs.jctc.0c00809

[6] A. Gottscholl, M. Kianinia, V. Soltamov, S. Orlinskii, G. Mamin, C. Bradac, C. Kasper, K. Krambrock, A. Sperlich, M. Toth, I. Aharonovich, V. Dyakonov. Nat. Mater. **19**, *5*, 540 (2020). DOI: 10.1038/s41563-020-0619-6

[7] W. Lee, V.S. Liu, Z. Zhang, S. Kim, R. Gong, X. Du, K. Pham, T. Poirier, Z. Hao, J.H. Edgar, P. Kim, C. Zu, E.J. Davis, N.Y. Yao. Phys. Rev. Lett. **134**, *9*, 096202 (2025). DOI: 10.1103/PhysRevLett.134.096202

[8] F.F. Murzakhanov, B.V. Yavkin, G.V. Mamin, S.B. Orlinskii, I.E. Mumdzhi, I.N. Gracheva, B.F. Gabbasov, A.N. Smirnov, V.Y. Davydov, V.A. Soltamov. Nanomaterials **11**, *6*, 1373 (2021). DOI: 10.3390/nano11061373

[9] G. Wolfowicz, F.J. Heremans, C.P. Anderson, S. Kanai, H. Seo, A. Gali, G. Galli, D.D. Awschalom. Nat. Rev. Mater. **6**, *10*, 906 (2021). DOI: 10.1038/s41578-021-00306-y

[10] G.D. Fuchs, G. Burkard, P.V. Klimov, D.D. Awschalom. Nature Phys. **7**, *10*, 789 (2011). DOI: 10.1038/nphys2026

[11] M.A. Perlin, Z. Wang, J. Casanova, M.B. Plenio. Quantum Sci. Technol. **4**, *1*, 015007 (2019). DOI: 10.1088/2058-9565/aade5c

[12] A. Bourassa, C.P. Anderson, K.C. Miao, M. Onizhuk, H. Ma, A.L. Crook, H. Abe, J. Ul-Hassan, T. Ohshima, N.T. Son, G. Galli, D.D. Awschalom. Nat. Mater. **19**, *12*, 1319 (2020). DOI: 10.1038/s41563-020-00802-6

[13] C.E. Bradley, J. Randall, M.H. Abobeih, R.C. Berrevoets, M.J. Degen, M.A. Bakker, M. Markham, D.J. Twitchen, T.H. Taminiau. Phys. Rev. X **9**, *3*, 031045 (2019). DOI: 10.1103/PhysRevX.9.031045

Translated by A.Akhtyamov